Author Manuscript

Author Manuscript

Author Manuscript

Author Manuscript

HHS Public Access

Author manuscript

Oncogene. Author manuscript; available in PMC 2014 July 30.

Published in final edited form as:

Oncogene. 2014 January 30; 33(5): 632–642. doi:10.1038/onc.2012.620.

Chromatin effector Pygo2 regulates mammary tumor initiation and heterogeneity in *MMTV-Wnt1* mice

Kazuhide Watanabe, **Magid Fallahi**, and **Xing Dai***

Department of Biological Chemistry, School of Medicine, University of California, Irvine, CA 92697

Abstract

Little is known about chromatin mechanisms that regulate tumor-initiating cells that are proposed to be responsible for tumor recurrence and relapse. We have previously shown that Pygopus 2 (Pygo2), a chromatin effector and context-dependent Wnt signaling co-activator, regulates mammary gland development by expanding epithelial stem/progenitor cells. However, the role of Pygo2 in mammary tumorigenesis in vivo remains to be addressed. In this study, we show that epithelia-specific ablation of *Pygo2* in *MMTV-Wnt1* transgenic mice results in delayed mammary ductal elongation, but the hyperbranching phenotype, aberrant accumulation of stem/progenitor-like cells, and canonical Wnt signaling output are largely unaffected. Chronic loss of Pygo2 significantly delays mammary tumor onset in *MMTV-Wnt1* females, whereas acute deletion of *Pygo2* in *MMTV-Wnt1* tumor cells leads to a significant decrease in their tumor initiating capability upon transplantation. Finally, we provide evidence supporting a role for Pygo2 in modulating the lineage potential of *MMTV-Wnt1* tumor initiating cells. Collectively, our results suggest that Pygo2 acts at a step downstream of mammary stem cell accumulation to facilitate transformation, and that it regulates the tumor initiating capacity and lineage preference of the already transformed mammary cells, in *MMTV-Wnt1* mice. These findings offer valuable insights into our understanding of the molecular basis of heterogeneity within breast tumors.

Keywords

MMTV-Wnt1; Pygopus 2; mammary gland; tumorigenesis; tumor heterogeneity; tumor-initiating cells; cancer stem cells

Users may view, print, copy, download and text and data- mine the content in such documents, for the purposes of academic research, subject always to the full Conditions of use: http://www.nature.com/authors/editorial_policies/license.html#terms

*To whom correspondence should be addressed: Department of Biological Chemistry, School of Medicine, D250 Med Sci I, University of California, Irvine, CA 92697-1700, Tel: 949-824-3101, Fax: 949-824-2688, xdai@uci.edu.

Disclosure of potential conflicts of interest: None.

CONFLICT OF INTEREST

The authors declare no conflict of interest.

SUPPLEMENTARY INFORMATION

Supplementary information accompanies the paper on the Oncogene website (http://www.nature.com/onc).

Author Manuscript Author Manuscript Author Manuscript Author Manuscript

INTRODUCTION

Tumor heterogeneity remains a major challenge to cancer therapy. The cancer stem cell hypothesis posits that a small subset of cells in a given tumor are capable of long-term self-renewal, generating multiple cell types that constitute a heterogeneous tumor, and initiating a new tumor that resembles the original one (hence also termed tumor-initiating cells) (1). Growing evidence suggests the existence of tumor-initiating cells in both leukemia and solid tumors including breast cancer (2, 3). However, our current understanding of the molecular pathways that regulate tumor-initiating cells is limited to a small number of signaling pathways and regulatory factors such as Wnt, Hh, Notch, and Bmi-1 (4–8). Identification of novel regulators will not only uncover basic mechanisms of cancer stem cell regulation, but also increase the repertoire of potential molecular targets for clinical intervention.

The Wnt/β-catenin signaling pathway is essential for myrid developmental processes including mammary gland (MG) development (9). Pygopus 2 (Pygo2) is a member of the Pygopus protein family initially discovered as a transcriptional co-activator of the Wnt/β-catenin pathway, but later found to also possess the ability to directly bind to histone H3 that is trimethylated at lysine 4 (H3K4me3) (10–15). Moreover, Pygo2 associates with histone-modifying enzymes and recruits them to target chromatin to facilitate H3K4 trimethylation and histone acetylation in normal mammary epithelial progenitor cells as well as breast cancer cell lines (15–18). Loss of Pygo2 results in defective MG morphogenesis accompanied by suboptimal expansion of developmental mammary epithelial progenitor cells, underscoring the importance of this histone-code reader in regulating normal tissue stem/progenitor cells (15). Up-regulated expression of Pygo2 has been reported in malignant tumors of several tissues including the breast (19). However, whether Pygo2 regulates tumorigenesis, particularly tumor-initiating cells, in vivo remains to be addressed.

Mammary tumors produced by *mouse mammary tumor virus (MMTV)-Wnt1* transgenic mice are histologically heterogeneous, containing multiple cell lineages within a single tumor (20–22). These tumors contain discrete population(s) of tumor initiating cells, unlike other tumor models such as *MMTV-ErbB2* in which all tumor cells exhibit similar tumor-initiating capacity (21, 23). Moreover, the preneoplastic mammary tissue in *MMTV-Wnt1* mice is highly enriched for stem/progenitor-like cells, including the mammary stem cell (MaSC)-enriched basal (MaSC/basal) cell population (24–26). As such, *MMTV-Wnt1* mice offer an ideal model to study the molecular regulation of cancer stem cells and the cell of origin of breast cancers (23, 27, 28). In the current work, we studied the impact of *Pygo2* deletion on *MMTV-Wnt1*-induced mammary outgrowth and tumorigenesis. We show that Pygo2 loss from the mammary epithelia exerts a context-dependent effect on stem/progenitor cells in the preneoplastic tissue, and dramatically delays tumor onset. We also provide evidence for a functional involvement of Pygo2 in regulating tumor initiation as well as lineage differentiation of *MMTV-Wnt1* tumor cells.

Author Manuscript Author Manuscript Author Manuscript Author Manuscript

RESULTS

Elevated expression of Pygo2 in *MMTV-Wnt1* MGs and tumors

Previous studies have reported elevated Pygo2 expression in human breast cancer cells (16, 19). Consistently, our interrogation of the publically available gene expression data (29) revealed a significantly elevated level of *Pygo2* mRNA in invasive ductal carcinoma samples compared with normal tissue controls (Supplemental Figure 1). To further explore the involvement of Pygo2 in tumorigenesis in vivo, we examined its expression in preneoplastic and tumorous mammary tissues from the *MMTV-Wnt1* mice. Quantitative RT-PCR analysis revealed elevated level of *Pygo2* mRNA in *MMTV-Wnt1* tumors, whereas mRNA up-regulation in the preneoplastic tissues was insignificant (Figure 1A). The level of Pygo2 protein was consistently higher in *MMTV-Wnt1* MGs than littermate controls, and was further elevated in *MMTV-Wnt1* tumors (Figure 1B, Supplemental Figure 2). As previously shown in wild-type MGs (15), Pygo2 protein was detected in nearly all luminal cells and a subset of basal/myoepithelial cells of the ducts, as well as in body cells and some cap cells of the terminal end buds (TEBs) of the *MMTV-Wnt1* MGs (Figure 1C, D). Moreover, a majority of the tumor cells from *MMTV-Wnt1* mice exhibited prominent presence of the Pygo2 protein (Figure 1C). Significant nuclear staining was also observed in the surrounding stromal cells (Figure 1C). Together, our findings suggest that elevated Pygo2 expression is an early hallmark of tumorigenesis in the *MMTV-Wnt1* model.

Pygo2 regulates the preneoplastic phenotype of *MMTV-Wnt1* MGs in a context-dependent manner

To examine whether Pygo2 is functionally involved in *MMTV-Wnt1*-induced overgrowth, we introduced *keratin 14 (K14)-Cre*-mediated conditional ablation of *Pygo2* (skin/mammary gland epithelia-specific knockout of *Pygo2; Pygo2* SSKO) (15) into the *MMTV-Wnt1* transgenic mice. K14 normally marks the multipotent progenitor cells of developing mammary epithelia and the basal population of the mature MG including the multipotent stem cells that are responsive to Wnt signals (24, 30). As such, *K14-Cre* can be used to inactivate luminally expressed genes (31), and its expression indeed resulted in recombination at the *ROSA26R* locus (32) in not only basal but also luminal epithelial cells of adult MG.(Supplemental Figure 3). Importantly, immunohistochemistry revealed depletion of Pygo2 protein expression from mammary epithelial cells but not from stromal cells of the *MMTV-Wnt1/Pygo2* SSKO mice, validating the targeting approach (Figure 1C).

MMTV-Wnt1-induced preneoplastic mammary phenotype arises early (apparent 2 weeks after birth) (20) and Pygo2 regulates MG morphogenesis (15). Therefore, we examined the genetic interaction between *MMTV-Wnt1* and *Pygo2* during postnatal MG development. The loss of epithelial Pygo2 did not rescue the hyperbranching phenotype of developing (3–8 weeks) *MMTV-Wnt1* MGs (Figure 2A–C, Supplemental Figure 4), or impact the MG branching morphology of aged *MMTV-Wnt1* virgin females (data not shown). Moreover, the phenotypes of smaller TEBs and delayed ductal elongation previously reported for *Pygo2* SSKO mice (15) were still observed in *MMTV-Wnt1*/*Pygo2* SSKO mice (Figure 2A, D, E, and Supplemental Figure 4). As in *Pygo2* SSKO mice, the ductal elongation phenotype was no longer present in mature MGs of *MMTV-Wnt1*/*Pygo2* SSKO mice that were 12 weeks or

Author Manuscript Author Manuscript Author Manuscript Author Manuscript

older (data not shown). Thus, Pygo2 deletion causes a transient retardation of mammary ductal elongation despite the presence of the *MMTV-Wnt1* transgene.

To further address any functional convergence between *MMTV-Wnt1* and *Pygo2*, we analyzed male *MMTV-Wnt1* mice where rudimentary MG development occurs without the influence of female hormones (33). Remarkably, *Pygo2* deletion rescued the abnormal mammary tree formation observed in *MMTV-Wnt1* males (Figure 2F, G). Therefore, Pygo2 is required for *MMTV-Wnt1*-induced mammary hyperbranching in a hormone-independent environment.

Pygo2 loss leads to a reduced number of TEB K6$^+$ progenitor cells, whereas the aberrant MaSC/basal cells in *MMTV-Wnt1* MGs still accumulated but showed altered gene expression

Characteristic cellular features of the preneoplastic *MMTV-Wnt1* MGs include aberrant accumulation of keratin 6 (K6)-expressing progenitor cells (25) and an expanded Lin$^-$ CD24$^+$CD29^{high} MaSC/basal population (24) (Figure 3A–C). We first compared the distribution of K6$^+$ cells in developing *MMTV-Wnt1* MGs with and without Pygo2. While normally K6$^+$ cells were concentrated in the TEBs but scattered in the ducts (34), the abundance of these cells was significantly increased in the ducts but decreased in the TEBs of *MMTV-Wnt1* MGs (Figure 3A, B). Furthermore, the *MMTV-Wnt1* ductal K6$^+$ cells often co-expressed basal marker K14 and luminal marker keratin 8 (K8) (Figure 3A, Supplemental Figure 5), suggestive of the accumulation of bipotent progenitor cells. Importantly, loss of Pygo2 did not affect the aberrant ductal progenitor cells, but resulted in a further decrease of TEB K6$^+$ cells in *MMTV-Wnt1* MGs (Figure 3A, B). An overall picture emerging from this and previous analyses (15) is that *MMTV-Wnt1* and Pygo2 regulate distinct but possibly overlapping progenitor cell pools, with *MMTV-Wnt1* preferentially stimulating the accumulation of ductal bipotent K6$^+$ progenitor cells, whereas Pygo2 preferentially regulating K6$^+$ progenitor cells in the TEB.

We also examined whether *MMTV-Wnt1* and *Pygo2* converge to regulate the Lin$^-$CD24$^+$CD29^{high} MaSC/basal population in adult MG (Figure 3C). Deletion of *Pygo2* did not affect the aberrant expansion of this population, nor did it affect the size of the Lin$^-$CD24$^+$CD29^{low}CD61^{high} luminal progenitor cell population (35), in *MMTV-Wnt1* MGs. Despite the apparently normal surface marker expression, we wondered whether the accumulated MaSC/basal cells in *MMTV-Wnt1* MGs might be affected in gene expression by Pygo2 loss. Towards this end, we performed DNA microarray analysis using fluorescence-activated cell sorting (FACS)-purified MaSC/basal cells from wild-type, *MMTV-Wnt1*, and *MMTV-Wnt1*/*Pygo2* SSKO MGs. This analysis revealed overall similar transcriptional profiles between *MMTV-Wnt1* and *MMTV-Wnt1*/*Pygo2* SSKO MaSC/basal cells (Supplemental Figure 6A). Using a stringent cut-off (fold change >2 and p value<0.05), only 331 and 22 genes were differentially expressed between wild type and *MMTV-Wnt1*, and between *MMTV-Wnt1* and *MMTV-Wnt1*/*Pygo2* SSKO populations, respectively (Supplemental Table 1). In addition, *Pygo2* loss did not exhibit a consistent effect on the expression of select Wnt target genes (Supplemental Figure 6B). With these said, Gene Set Enrichment Analysis (GSEA) detected significant alterations in specific

Author Manuscript Author Manuscript Author Manuscript Author Manuscript

signature gene sets (Figure 3D). Of note, genes involved in cell cycle/proliferation control and chromosome regulation were enriched in *MMTV-Wnt1*, whereas genes involved in extracellular matrix/cell adhesion were enriched in *MMTV-Wnt1*/*Pygo2* SSKO MaSC/basal cells.

Loss of epithelial Pygo2 delays mammary tumor onset in *MMTV-Wnt1* mice

In contrast to the lack of a strong effect on hyperbranching, *Pygo2* deletion significantly delayed the onset of mammary tumors in female *MMTV-Wnt1* mice, with 50% tumor-free survival being extended from 225 days in *MMTV-Wnt1* to 492 days in *MMTV-Wnt1*/*Pygo2* SSKO mice (p=0.007 by Log-rank test) (Figure 4A). The mixed strain background used in this study did not significantly affect tumor incidence in *MMTV-Wnt1* mice (Figure 4A). Tumors that did form in *MMTV-Wnt1*/*Pygo2* SSKO mice were largely composed of Pygo2-negative cells, with Pygo2 signal being detected only in the stromal compartment (Figure 4B), and showed variable growth rate with no consistent difference from the controls (data not shown). Furthermore, tumor cells isolated from the *MMTV-Wnt1* and *MMTV-Wnt1*/*Pygo2* SSKO mice did not demonstrate any consistent difference in tumor growth upon transplantation (data not shown).

MMTV-Wnt1-derived tumors are generally adenocarcinomas with heterogeneous cell types and most of tumor cells can be roughly categorized into a mixture of the following histological types: papillary/ductal, microaciner (cribriform), and adenosquamous (22). Distribution of cell types was similar between genotypes, with papillary/ductal and microaciner types being the majority and no clear difference in the expression pattern of luminal and basal keratin markers K8 and K14 in well-differentiated papillary/ductal regions of the tumors (Supplemental Figure 7 and data not shown).

In vivo and in vitro analysis reveals minimal impact of Pygo2 loss on canonical Wnt signaling in *MMTV-Wnt1* mammary cells

We next asked whether *Pygo2* deletion affects Wnt signaling output in *MMTV-Wnt1* MGs.. Specifically, we introduced a commonly used Wnt reporter, the *Axin2*^{LacZ}allele (36), into the *MMTV-Wnt1*/*Pygo2* SSKO mice. Using X-gal staining, we detected similar reporter activities in whole-mount *MMTV-Wnt1* MGs despite whether the *Pygo2* gene was intact or not (Figure 5A). Strong activity was detected in the basal layer as well as in some luminal cells of both *MMTV-Wnt1* and *MMTV-Wnt1*/*Pygo2* SSKO MGs (Figure 5A, B). To better quantify reporter activity, we performed FACS analysis using a fluorescent LacZ substrate along with antibodies against cell surface antigens (CD24, CD29 and lineage markers) (Figure 5C). Reporter expression was normally detected in the Lin^{-}CD24^{+}CD29^{high} MaSC/basal cells but not Lin^{-}CD24^{+}CD29^{low} luminal cells (Figure 5C). In *MMTV-Wnt1* MGs, however, reporter expression was dramatically elevated in the luminal cells to a level comparable to that in the MaSC/basal cells (Figure 5C). Our finding is consistent with a recent report detecting *Axin2*^{LacZ} reporter activity and *Axin2* mRNA in both basal and luminal compartments (37), but contrasts two earlier reports of Wnt activity exclusively in the MaSC/basal cells of *MMTV-Wnt1* MGs (27, 28). This discrepancy may arise from the use of different detection methods, with the former studies employing quantitative assays whereas the latter studies relying solely on a histological evaluation of LacZ-positive cells

Author Manuscript Author Manuscript Author Manuscript Author Manuscript

which might not have been sufficiently sensitive. Importantly, deletion of *Pygo2* did not significantly affect reporter activity in either MaSC/basal or luminal populations of the *MMTV-Wnt1* MGs (Figure 5C).

To assess the effect of Pygo2 loss on canonical Wnt signaling in tumor cells, we established a heterogeneous tumor cell line (G236) from a *MMTV-Wnt1*/*Pygo2*$^{flox/-}$ mouse (see Materials and Methods) and examined the effect of *Pygo2* deletion on Wnt signaling activity in these cells. Addition of recombinant Wnt3a protein led to a dose-dependent increase in signaling activity as assayed by the super-TOP-Flash (LEF/TCF reporter)/FOP (mutated LEF/TCF reporter) ratio (Figure 5D), indicating that G236 cells are capable of transmitting Wnt signaling. Loss of Pygo2 upon infection with Cre-expressing adenoviruseses (Ad-Cre; Ad-GFP was used as a control) (Figure 5E) led to an increase of basal, but decrease of Wnt3a-stimulated, reporter gene expression (Figure 5D). Overall, although the dose response curve was less steep than control, Pygo2-deficient cells still responded to Wnt ligand stimulation. Collectively, these results raise the interesting possibility that Pygo2 acts in Wnt-induced tumorigenesis via both Wnt-dependent and Wnt-independent mechanisms.

Acute deletion of *Pygo2* in pre-existing *MMTV-Wnt1* tumor cells results in reduced tumor-initiating frequency and altered lineage potential

To test whether Pygo2 regulates the functional cancer stem cell pool, we isolated primary tumor cells from *MMTV-Wnt1*/*Pygo2*$^{flox/-}$ mice, infected them with Ad-GFP or Ad-Cre, and monitored the ability of the infected cells to produce tumorspheres in culture and to initiate tumors upon transplantation onto nude mice (Figure 6A). GFP expression was used to monitor adenoviral infection efficiency and shown to correlate well with loss of the Pygo2 protein (Supplemental Figure 8A, B). Comparing to Ad-GFP-infected cells (~95% GFP-positive), Ad-Cre-infected cells (~85% GFP-positive; Supplemental Figure 8A) showed dramatically impaired ability to initiate new tumorspheres upon passaging (Figure 6B). Moreover, in transplantation experiments, Ad-Cre-infected cells at limiting dilutions showed greatly reduced tumor take rates comparing to Ad-GFP-infected cells (Figure 6C). Calculation of tumor-initiating frequency revealed a >10-fold reduction upon acute *Pygo2* deletion (Figure 6C).

Remarkably, of the 17 tumors derived from Ad-Cre-infected cells in three independent transplantation experiments, a vast majority (15 out of 17; 88%) contained abundant cells that expressed Pygo2, even though >80% of the cells were devoid of Pygo2 at the time of transplantation (Figure 7A, B, Supplemental Figure 8A). Among these, six (35%) tumors, which showed a well-differentiated ductal/papillary morphology with both basal and luminal cell constituents, were populated entirely by Pygo2-expressing cells (Figure 7A, left). This result suggests that Pygo2 expression may confer selective growth advantage to tumor-initiating cells during tumor progression.

Nine (53%) tumors contained a mixture of Pygo2-positive cells (60.2±11.9%, as estimated by random sampling of 10 “mixed regions” from four different sections) and Pygo2-negative cells (Figure 7A, middle, and 7B). A majority of these mixed-type tumors displayed papillary/ductal-type histology with a few unclassified/undifferentiated regions (data not shown). The incidence of such mixed-type tumors increased with the increasing

Author Manuscript Author Manuscript Author Manuscript Author Manuscript

number of transplanted tumor cells (Figure 7C), suggesting that injection of more cells allowed the generation of polyclonal tumors where both Pygo2-expressing (uninfected) and Pygo2-deficient (Ad-Cre infected) participated in tumor formation. Interestingly, Pygo2-positive and Pygo2-negative cells were often distinctly partitioned into luminal and basal, respectively, compartments or vice versa (Figure 7D and data not shown), as if they each arose as clones of lineage-restricted basal or luminal progenitor cells. Again, the abundance of Pygo2 expression in these tumors suggests the competitive advantage of Pygo2-expressing tumor cells in supporting tumor growth. Only in rare cases did we observe contribution of Pygo2-deficient cells to both basal and luminal cell types within a small ductal/papillary region, suggesting that tumor-initiating cells may have restricted lineage potential in the absence of Pygo2.

Only 2 (12%) tumors were populated entirely by Pygo2-deficient epithelial cells (Figure 7B). Interestingly, these tumors showed an exclusively microacinar-type histology (Supplemental Figure 9). In addition, Pygo2-deficient regions in the mixed-type tumors were frequently found to associate with tumor sub-regions that presented a microacinar morphology (Figure 7E). These results raise the intriguing possibility that loss of Pygo2 favors tumorigenesis from alveolar progenitor cells, and/or promotes the differentiation of tumor-initiating cells towards an alveolar fate. Collectively, our findings suggest an important role for Pygo2 in enabling multipotent stem and lineage-restricted progenitor cells to initiate new tumors as well as in specifying tumor histology/subtypes.

Finally, we tested the effect of pyrvinium, a recently reported compound that blocks canonical Wnt activity partially through promoting casein kinase 1α activation and proteasomal degradation of the Pygo2 protein (38). Intraperitoneal administration of 0.5 mg/kg/day pyrvinium pamoate to nude mice, which had been transplanted with the *MMTV-Wnt1* primary tumor cells (Figure 8A), indeed slowed down tumor growth (Figure 8B). We were not able to test higher doses of pyrvinium pamoate due to its side effects including a slight, but significant suppression of total body weight (Supplemental Figure 10). This said, our proof-of-principle data suggest that chemically targeting Pygo2 and its associated Wnt signaling pathway affects tumor progression in vivo.

DISCUSSION

In the current work, we describe for the first time an important role for Pygo2 in Wnt-induced mammary tumorigenesis. Chronic and acute deletion of *Pygo2* suppressed the onset and tumor-reinitiating activity of *MMTV-Wnt1*-induced tumors, respectively. Previous in vitro studies have shown that siRNA-mediated knockdown of Pygo2 results in decreased presence of a subpopulation of human breast cancer cells that express cancer stem cell markers (16). This study presents the first in vivo, functional evidence that Pygo2 regulates both the initiation and lineage differentiation of mammary tumors.

Our data present new insights into the molecular control of mammary tissue stem/progenitor cells and the specific roles of Wnt signaling. In contrast to its strong impact on *MMTV-Wnt1*-induced tumorigenesis, the effect of Pygo2 loss on Wnt signaling-induced mammary overgrowth is manifest only in some contexts: the precocious branching and lateral bud

Author Manuscript Author Manuscript Author Manuscript Author Manuscript

formation in MGs of *K14-ΔN-β-catenin* females and the abnormal growth of MGs in *MMTV-Wnt1* males are rescued [(15); this work], whereas the extensive ductal hyperbranching in MGs of *MMTV-Wnt1* females is not (this work). It is formally possible that the different strain backgrounds of the *K14-ΔN-β-catenin* vs. *MMTV-Wnt1* mice used in our analyses account for such phenotypic difference. This said, we did not observe any significant difference between a mixed background and pure FVB/N background for the preneoplastic phenotypes or tumor incidence of *MMTV-Wnt1* mice (Figure 4A and data not shown). Instead, the differential rescue may be explained by a β-catenin/Pygo2-independent effect of the *MMTV-Wnt1* transgene, such as triggering activation of noncanonical Wnt signaling pathways. In addition, different target populations of active Wnt signaling between the two models as well as between females and males might account for their different Pygo2 dependency. Canonical Wnt signaling is activated in basal cells of the *K14-ΔN-β-catenin* MGs, whereas Wnt-responsive cells are found in both basal and luminal compartments of the MGs of *MMTV-Wnt1* females [(37); this study]. Thus, these Wnt-responsive populations do not completely overlap with sites of Pygo2 expression, which include predominantly luminal cells but also some basal cells. The target population in MGs of *MMTV-Wnt1* males has not been determined in our study. Interestingly, the impaired TEB formation and transient delay in ductal elongation caused by *Pygo2* deletion in wild-type MGs (15) still occurs in *MMTV-Wnt1* MGs. Taken together with the differential effect of *MMTV-Wnt1* and *Pygo2* deletion on ductal vs. TEB progenitor cells, these data are consistent with different subpopulations of progenitor cells being responsible for ductal branching vs. elongation during mammary development (5, 39). Finally, the loss of Pygo2 might also exert a systemic, non-cell autonomous effect, such as altering sex hormone levels or modifying specific responses to hormones (40), thereby modifying the Wnt transgenic phenotypes. Future studies will be needed to further explore these possibilities.

Our data are consistent with Pygo2 acting downstream of the initial expansion of mammary tissue stem/progenitor cells to facilitate malignant transformation. It is possible that Wnt1 stimulates the self-renewal of the stem/progenitor cells whereas Pygo2 facilitates their subsequent proliferation which allows tumorigenic mutations to occur and accumulate. The Pygo2 deficiency-induced alteration in cell cycle gene expression supports this notion. Our gene expression and reporter analysis of preneoplastic *MMTV-Wnt1* MGs revealed little or no detectable alteration in canonical Wnt signaling upon Pygo2 loss. Moreover, Pygo2 loss elicits opposite in vitro effects on the basal and activated canonical Wnt signaling in G236 tumor cells. Thus, Pygo2's action as a chromatin effector (10–15) goes beyond simply facilitating Wnt signaling, a notion that is consistent with the *Pygo2* knockout phenotypes presented in the current and previous reports (15, 41, 42). Further studies outside the scope of this work will be needed to identify unknown molecular event(s) that is regulated by Pygo2.

The relationship between the cell of origin of a particular tumor and its cancer stem cells remains ill-defined (43). Our study now suggests that they are both under the control of Pygo2, as Pygo2 loss not only delayed the onset of primary *MMTV-Wnt1* tumors, but also reduced the frequency of tumor-initiating cells in preexisting tumors. In an elegant study of the gene expression profiles of mammary tumors from various mouse models, tumors from

Author Manuscript Author Manuscript Author Manuscript Author Manuscript

MMTV-Wnt1 mice were found to fall into two distinct groups (III and IV) that both display basal/myoepithelial features (44). A main characteristics of the *MMTV-Wnt1* tumors, as uncovered by this and other studies, is the presence of heterogeneous cell types and expression of both luminal and basal/myoepithelial gene clusters. Interestingly, Pygo2-deficient cells were able to contribute to *MMTV-Wnt1* tumors with this characteristic heterogeneity (21, 23) only when Pygo2-expressing cells were also present. On the other hand, tumors completely devoid of Pygo2-expressing cells lost this heterogeneity and were predominantly of the microacinar subtype. These data suggest that 1) Pygo2-expressing tumor cells orchestrate the production of heterogeneous tumors and may exert paracrine effects on Pygo2-deficient cells to modify their behavior; 2) Pygo2-deficient tumor-initiating cells when standing alone are more restricted in their lineage differentiation potential and can only, for example, serve as alveolar progenitor cells. Along this line, it is intriguing to speculate that the presence of Pygo2 may promote the lineage plasticity of cancer stem cells (45), a notion worthy of future investigation.

In contrast to findings from transplantation studies where *Pygo2* was acutely deleted, we did not observe any obvious lineage restriction of Pygo2-null tumor cells in the chronic deletion model. This discrepancy may be explained by possible additional genetic mutations or epigenetic alterations that occur in the chronic model, yielding compensatory and/or alternative molecular mechanisms that allow Pygo2-independent tumor growth. In the acute deletion-transplantation model, there may not be sufficient time to allow such adaptive changes to occur, hence allowing the manifestation of a dependence of the resulting tumors on Pygo2 for their initiation and maintenance.

In our study, *Pygo2* deletion exerts a significant effect on tumorigenesis in the MMTV-Wnt1 animal model, extending the 50% tumor-free survival by 267 days. This length of time represents 37% of the typical life span of laboratory mice, which is about 2 years. Thus, it is reasonable to consider the Pygo2-related pathway as a possible candidate for targeted therapeutics in breast cancer prevention and treatment. Further supporting this notion, Pygo2 loss has a remarkable effect on tumorigenesis in the acute deletion-transplantation model, both by reducing the frequency of the tumor initiating cells, and by altering their lineage differentiation potential. Thus, it might be of interest to explore the targeting of Pygo2 expression or function as adjuvant, “differentiation” therapeutics to promote the differentiation of breast cancer stem cells, which are proposed to be responsible for cancer recurrence and relapse (2). Although pyrvinium treatment can cause a significant reduction in tumor growth in the *MMTV-Wnt1* model, the effectiveness of the drug is limited because of side effects. Thus, identification and generation of more specific and less toxic compounds may be necessary to pursue the potential therapeutic effect of inhibiting Pygo2 and its associated Wnt signaling pathway in vivo.

MATERIALS AND METHODS

Generation of *MMTV-Wnt1/Pygo2* SSKO mice

Generation and genotyping of null and floxed *Pygo2* alleles were as previously described (15, 46). *MMTV-Wnt1* mice were a gift of Yi Li’s laboratory. *Axin2*$^{LacZ/+}$ (B6.129P2-*Axin2*^{tm1Wbm}/J) and *Rosa26R* (B6.129S4-*Gt(ROSA)26Sor*^{tm1Sor}/J) mice were purchased

Author Manuscript Author Manuscript Author Manuscript Author Manuscript

from the Jackson Laboratory. *Axin2*$^{LacZ/+}$/*MMTV-Wnt1*/*Pygo2* SSKO mice were generated in an FVB/N and C57BL/6-mixed background (62.5% FVB/N and 37.5% B6 for *MMTV-Wnt1*/*Pygo2* SSKO; 56.25% FVB/N and 43.75% B6 for *Axin2*$^{LacZ/+}$/*MMTV-Wnt1*/*Pygo2* SSKO) by crossing *Axin2*$^{LacZ/+}$/*MMTV-Wnt1*/*K14-Cre*/*Pygo2*$^{+/-}$ males with *Pygo2*$^{flox/flox}$ females. Tumor-free survival for *MMTV-Wnt1* mice in this mixed background was similar to that in a pure FVB/N background (20) (Figure 4A and data not shown). All experiments have been approved by and conform to the regulatory guidelines of the International Animal Care and Use Committee of the University of California, Irvine.

Morphology, immunostaining and Western blot analysis

For whole-mount MG staining, MGs (#3 or #4) were dissected, fixed overnight in Carnoy's solution (60% ethanol, 30% chloroform, and 10% glacial acetic acid), and stained with carmine alum as previously described (15). X-gal staining was performed as previously described (37). For histological analysis, MGs were fixed in 4% paraformaldehyde in phosphate-buffered saline (PBS), washed, embedded in paraffin, sectioned, and stained with hemotoxylin and eosin (H/E).

Immunohistochemical detection of Pygo2 (46), K8 (rat; 1:1000; Developmental Studies Hybridoma Bank), K19 (rat; 1:1000, Developmental Studies Hybridoma Bank), K5 (rabbit 1:1000), K6 (rabbit; 1:1000), K14 (rabbit; 1:2,000) (K5, K6 and K14 antibodies were gifts from J. Segre, National Institutes of Health, Bethesda, MD), Ki67 (Vector Laboratories, VP-K451; 1:500) was performed with paraformaldehyde-fixed OCT sections, using Vector ABC (Vector Laboratories, PK-6100) and DAB (DAKO, K3468) kits according to manufacturers' recommendations. Antigen-retrieval was performed by incubating slides in Tris-EDTA buffer (pH 9.0) in microwave for 20 min. Indirect immunofluorescence of K8, K19, K5, K6, and K14 was performed as previously described (47). Western blot analysis was performed as previously described (15) using antibodies including anti-Pygo2 (46) and anti-β-actin (Sigma). Proteins were collected from the isolated mammary cell pellets as described in FACS analysis (see below). Blots were subjected to densitmetric analysis using the Multi Gauge V3.0 software (Fujifilm). Pygo2 levels were normalized against β-actin levels and further corrected for the epithelial contents as revealed by FACS analysis (Supplemental Figure 1).

FACS analysis and live cell sorting

MGs (#3–5) or tumors were surgically isolated form adjacent tissues, minced into 1 mm fractions and digested for 2–4 h at 37°C in DMEM/F12 containing 5% fetal bovine serum (FBS), 300 U/ml collagenase (Sigma Aldrich), and 100 U/ml hyaluronidase (Sigma Aldrich) with shaking at 200 rpm. After vortexing and lysis of the red blood cells in ammonium chloride, a single-cell suspension was obtained by sequential dissociation of the fragments by gentle pipetting for 2 min in 0.25% trypsin and then for 2 min in 5 mg/ml dispase II (STEMCELL Technologies Inc.) plus 0.1 mg/ml DNase I (Sigma Aldrich) followed by filtration through a 40-mm mesh. For all mammary cell isolations, viable cells were counted on a hemacytometer using Trypan blue exclusion.

Author Manuscript Author Manuscript Author Manuscript Author Manuscript

Staining was performed using the following antibodies and reagents: allophycocyanin (APC)-labeled anti-CD31 (BD), APC-labeled anti-CD45 (BD), APC-labeled anti-TER119 (BD), phycoerythrin (PE)/Cy7-labeled anti-CD24 (BD), FITC or PE-labeled anti-CD29 (BioLegened), PE-labeled anti-CD61 (BioLegend). Detection of LacZ activity using the fluorescent substrate di-D-β-galactopyranoside (FDG) was as described (48), with cells co-stained by PE/Cy7-labeled anti-CD24, PE-labeled anti-CD29, and APC-labeled lineage markers (CD31, CD45 and TER119). Cells were acquired on FACSCalibur (BD), and analysis was performed using FlowJo (Tree Star, Inc.). Live cell sorting was performed on a BD FACSAria equipped with FACS DiVa6.0 software operating at low pressure (20 psi) using a 100-μm nozzle. Cells were routinely double sorted and post-sort analysis typically indicated purities of >90% with minimal cell death (<10%).

RNA isolation and microarray analysis

Total RNA was isolated from freshly sorted $Lin^{-}CD24^{+}CD29^{high}$ MaSC/basal cells using the RNeasy mini kit (Qiagen). Hybridization of arrays (GeneChip Human Gene 1.0 ST, 901086, Affymetrix) was performed at the UCI Genomics High Throughput Facility (GHTF). Two biological replicates were performed for pooled RNA from at least 3 mice per genotype. Genes with normalized expression levels over detection threshold were called and analyzed for differential expression using the Cyber-T program (http://cybert.ics.uci.edu/). GSEA was performed using a Web-based tool (http://www.broadinstitute.org/gsea) based on previous publications (49).

Reverse-transcription and quantitative PCR (RT-qPCR)

cDNA was prepared using Retroscript high capacity cDNA reverse transcription kit (4368814, Applied Biosystems) according to manufacturer's instructions. Quantitative PCR was performed using a CFX96 qPCR system and SsoAdvanced SYBR Green supermix (Bio-rad). Primers used for gene expression analysis are: *Pygo2*, forward 5′-aggcagcccctctacttagc-3′, reverse 5′-ccaacccactttcttccaaa-3′ and *Gapdh*, forward 5′-aatgtgtccgtcgtggatct-3′, reverse 5′-ccctgttgctgtagccgtat-3′.

Acute deletion of *Pygo2*

Adenoviral transduction of Cre-recombinase was performed as described previously (50). Freshly isolated tumor cells from *MMTV-Wnt1*/$Pygo2^{flox/-}$ mice were incubated in suspension with control adenoviruses [Ad-IRES-GFP (Ad-GFP), Vector Biolab] or adenoviruses expressing Cre recombinase [Ad-Cre-IRES-GFP (Ad-Cre), Vector Biolab] at a multiplicity of infection (MOI) of 50 for 1 hour at 37°C. Cells were then washed with PBS and used immediately for tumorsphere culture or transplantation.

Serial dilution transplantation

After adenoviral infection, tumor cells were counted and resuspended in a 1:1 solution of PBS/Matrigel (BD). Ten μl each of limiting dilutions of control and experimental cells were injected into contralateral fat pads of #4 MGs of 6–8-week old athymic NCr-nu/nu mice (NU/J, Jackson Laboratory) that were anesthetized by an i.p. injection of ketamine and xylazine (750 and 50 mg/kg body weight, respectively). Tumor development was monitored

Author Manuscript Author Manuscript Author Manuscript Author Manuscript

for up to 4 months after transplantation. Statistical analysis of the take rate was performed using the ELDA Web-based tool (http://bioinf.wehi.edu.au/software/elda/) (51).

Tumorsphere assay

Tumorsphere assay was performed as previously described (52). After adenoviral infection, 5×10^4 tumor cells were seeded onto 24-well Ultra Low Attachment plates (Corning, Corning, NY) in DMEM/F12 (Invitrogen) supplemented with 20 ng/mL EGF, 40 ng/mL FGF-2, 5 μg/mL insulin, 0.5 μg/mL hydrocortisone, B27 (Invitrogen) and 4 ng/mL heparin. Tumorspheres were passaged every 7 days by mechanistically disaggregating with a 23-gauge needle followed by digestion with 0.25% trypsin for 3 min at 37°C. Five thousand cells were seeded for the second and third passages. Tumor spheres larger than 50 μm in diameter were counted.

Establishment of an *MMTV-Wnt1* tumor cell line (G236) and luciferase assay

G236 tumor cell line was established as a bulk population of tumor cells from a *MMTV-Wnt1*/*Pygo2*$^{flox/-}$ mouse using previously described method (53), and maintained in DMEM/F12 (Invitrogen) supplemented with 10% FBS, 20 ng/mL EGF, insulin and hydrocortisone (Sigma-Aldrich). G236 culture includes heterogeneous cell subpopulations and expresses both basal and luminal markers (data not shown).

For luciferase assay, G236 cells in 24-well plates were treated with Ad-GFP or Ad-Cre (see above) and transiently transfected with the SuperTOP/FOP-Flash constructs (200 ng/well). β-actin-LacZ (10 ng/well) was included as a transfection control. Wnt3a recombinant protein (R&D Systems, 5036-WN/CF) was added four hours after transfection. Cells were harvested 24 hours after the addition of Wnt3a, and luciferase activity was measured in whole cell extracts using the luciferase assay system (Promega). β-Galactosidase activity was measured as previously described (54).

Supplementary Material

Refer to Web version on PubMed Central for supplementary material.

Acknowledgments

We thank the UCI Genomics High Throughput Facility (GHTF) and Sue and Bill Gross Stem Cell Research Center Core Facility for expert service, Yi Li and Julie Serge for the generous gifts of *MMTV-Wnt1* mice and keratin antibodies, respectively, and Eva Lee for discussions. This work was supported by Susan G. Komen grant KG110897 and NIH Grant R01-GM083089 (to X.D.). K. W. was supported by a U.S. Department of Defense Breast Cancer Research Program (DOD BCRP) Postdoctoral Fellowship (W81XWH-10-1-0383).

ABBREVIATIONS

FACS	Fluorescence-activated cell sorting
GSEA	Gene Set Enrichment Analysis
H3K4me3	Histone H3 Lysine 4 trimethylation
H/E	Hemotoxylin and eosin

Author Manuscript Author Manuscript Author Manuscript Author Manuscript

MaSC	Mammary stem cell
MG	Mammary gland
MMTV	Mouse mammary tumor virus
PBS	phosphate-buffered saline
Pygo2	Pygopus 2
SSKO	Skin/mammary epithelia-specific knockout

References

1. Clevers H. The cancer stem cell: premises, promises and challenges. Nature medicine. 2011; 17(3): 313–9.
2. Visvader JE, Lindeman GJ. Cancer stem cells in solid tumours: accumulating evidence and unresolved questions. Nat Rev Cancer. 2008; 8(10):755–68. [PubMed: 18784658]
3. Bonnet D, Dick JE. Human acute myeloid leukemia is organized as a hierarchy that originates from a primitive hematopoietic cell. Nature medicine. 1997; 3(7):730–7.
4. Gu B, Watanabe K, Dai X. Epithelial stem cells: an epigenetic and Wnt-centric perspective. Journal of cellular biochemistry. 2010; 110(6):1279–87. [PubMed: 20564229]
5. Visvader JE. Keeping abreast of the mammary epithelial hierarchy and breast tumorigenesis. Genes & development. 2009; 23(22):2563–77. [PubMed: 19933147]
6. Raaphorst FM. Self-renewal of hematopoietic and leukemic stem cells: a central role for the Polycomb-group gene Bmi-1. Trends in immunology. 2003; 24(10):522–4. [PubMed: 14552834]
7. Jagani Z, Dorsch M, Warmuth M. Hedgehog pathway activation in chronic myeloid leukemia. Cell cycle (Georgetown, Tex. 2010; 9(17):3449–56.
8. Khalil S, Tan GA, Giri DD, Zhou XK, Howe LR. Activation status of Wnt/ss-catenin signaling in normal and neoplastic breast tissues: relationship to HER2/neu expression in human and mouse. PloS one. 2012; 7(3):e33421. [PubMed: 22457761]
9. Tepera SB, McCrea PD, Rosen JM. A beta-catenin survival signal is required for normal lobular development in the mammary gland. Journal of cell science. 2003; 116(Pt 6):1137–49. [PubMed: 12584256]
10. Kramps T, Peter O, Brunner E, et al. Wnt/wingless signaling requires BCL9/legless-mediated recruitment of pygopus to the nuclear beta-catenin-TCF complex. Cell. 2002; 109(1):47–60. [PubMed: 11955446]
11. Thompson B, Townsley F, Rosin-Arbesfeld R, Musisi H, Bienz M. A new nuclear component of the Wnt signalling pathway. Nature cell biology. 2002; 4(5):367–73. [PubMed: 11988739]
12. Belenkaya TY, Han C, Standley HJ, et al. pygopus Encodes a nuclear protein essential for wingless/Wnt signaling. Development (Cambridge, England). 2002; 129(17):4089–101.
13. Parker DS, Jemison J, Cadigan KM. Pygopus, a nuclear PHD-finger protein required for Wingless signaling in Drosophila. Development (Cambridge, England). 2002; 129(11):2565–76.
14. Fiedler M, Sanchez-Barrena MJ, Nekrasov M, et al. Decoding of methylated histone H3 tail by the Pygo-BCL9 Wnt signaling complex. Molecular cell. 2008; 30(4):507–18. [PubMed: 18498752]
15. Gu B, Sun P, Yuan Y, et al. Pygo2 expands mammary progenitor cells by facilitating histone H3 K4 methylation. The Journal of cell biology. 2009; 185(5):811–26. [PubMed: 19487454]
16. Chen J, Luo Q, Yuan Y, et al. Pygo2 associates with MLL2 histone methyltransferase and GCN5 histone acetyltransferase complexes to augment Wnt target gene expression and breast cancer stem-like cell expansion. Mol Cell Biol. 2010; 30(24):5621–35. [PubMed: 20937768]
17. Andrews PG, He Z, Popadiuk C, Kao KR. The transcriptional activity of Pygopus is enhanced by its interaction with cAMP-response-element-binding protein (CREB)-binding protein. Biochem J. 2009; 422(3):493–501. [PubMed: 19555349]

Author Manuscript Author Manuscript Author Manuscript Author Manuscript

18. Gu B, Watanabe K, Dai X. Pygo2 regulates histone gene expression and H3 K56 acetylation in human mammary epithelial cells. Cell cycle (Georgetown, Tex. 2011; 11(1)
19. Andrews PG, Lake BB, Popadiuk C, Kao KR. Requirement of Pygopus 2 in breast cancer. International journal of oncology. 2007; 30(2):357–63. [PubMed: 17203217]
20. Li Y, Hively WP, Varmus HE. Use of MMTV-Wnt-1 transgenic mice for studying the genetic basis of breast cancer. Oncogene. 2000; 19(8):1002–9. [PubMed: 10713683]
21. Vaillant F, Asselin-Labat ML, Shackleton M, Forrest NC, Lindeman GJ, Visvader JE. The mammary progenitor marker CD61/beta3 integrin identifies cancer stem cells in mouse models of mammary tumorigenesis. Cancer research. 2008; 68(19):7711–7. [PubMed: 18829523]
22. Munn RJ, Webster M, Muller WJ, Cardiff RD. Histopathology of transgenic mouse mammary tumors (a short atlas). Seminars in cancer biology. 1995; 6(3):153–8. [PubMed: 7495983]
23. Lindeman GJ, Visvader JE. Insights into the cell of origin in breast cancer and breast cancer stem cells. Asia-Pacific journal of clinical oncology. 2010; 6(2):89–97. [PubMed: 20565420]
24. Shackleton M, Vaillant F, Simpson KJ, et al. Generation of a functional mammary gland from a single stem cell. Nature. 2006; 439(7072):84–8. [PubMed: 16397499]
25. Li Y, Welm B, Podsypanina K, et al. Evidence that transgenes encoding components of the Wnt signaling pathway preferentially induce mammary cancers from progenitor cells. Proceedings of the National Academy of Sciences of the United States of America. 2003; 100(26):15853–8. [PubMed: 14668450]
26. Liu BY, McDermott SP, Khwaja SS, Alexander CM. The transforming activity of Wnt effectors correlates with their ability to induce the accumulation of mammary progenitor cells. Proceedings of the National Academy of Sciences of the United States of America. 2004; 101(12):4158–63. [PubMed: 15020770]
27. Baker R, Kent CV, Silbermann RA, Hassell JA, Young LJ, Howe LR. Pea3 transcription factors and wnt1-induced mouse mammary neoplasia. PloS one. 2010; 5(1):e8854. [PubMed: 20107508]
28. Teissedre B, Pinderhughes A, Incassati A, Hatsell SJ, Hiremath M, Cowin P. MMTV-Wnt1 and -DeltaN89beta-catenin induce canonical signaling in distinct progenitors and differentially activate Hedgehog signaling within mammary tumors. PloS one. 2009; 4(2):e4537. [PubMed: 19225568]
29. Zhao H, Langerod A, Ji Y, et al. Different gene expression patterns in invasive lobular and ductal carcinomas of the breast. Molecular biology of the cell. 2004; 15(6):2523–36. [PubMed: 15034139]
30. Van Keymeulen A, Rocha AS, Ousset M, et al. Distinct stem cells contribute to mammary gland development and maintenance. Nature. 2011; 479(7372):189–93. [PubMed: 21983963]
31. Derksen PW, Liu X, Saridin F, et al. Somatic inactivation of E-cadherin and p53 in mice leads to metastatic lobular mammary carcinoma through induction of anoikis resistance and angiogenesis. Cancer cell. 2006; 10(5):437–49. [PubMed: 17097565]
32. Soriano P. Generalized lacZ expression with the ROSA26 Cre reporter strain. Nature genetics. 1999; 21(1):70–1. [PubMed: 9916792]
33. Tsukamoto AS, Grosschedl R, Guzman RC, Parslow T, Varmus HE. Expression of the int-1 gene in transgenic mice is associated with mammary gland hyperplasia and adenocarcinomas in male and female mice. Cell. 1988; 55(4):619–25. [PubMed: 3180222]
34. Smith GH, Mehrel T, Roop DR. Differential keratin gene expression in developing, differentiating, preneoplastic, and neoplastic mouse mammary epithelium. Cell Growth Differ. 1990; 1(4):161–70. [PubMed: 1707299]
35. Asselin-Labat ML, Sutherland KD, Barker H, et al. Gata-3 is an essential regulator of mammary-gland morphogenesis and luminal-cell differentiation. Nature cell biology. 2007; 9(2):201–9. [PubMed: 17187062]
36. Lustig B, Jerchow B, Sachs M, et al. Negative feedback loop of Wnt signaling through upregulation of conductin/axin2 in colorectal and liver tumors. Molecular and cellular biology. 2002; 22(4):1184–93. [PubMed: 11809809]
37. Kim S, Goel S, Alexander CM. Differentiation generates paracrine cell pairs that maintain basaloid mouse mammary tumors: proof of concept. PloS one. 2011; 6(4):e19310. [PubMed: 21541292]

Author Manuscript Author Manuscript Author Manuscript Author Manuscript

38. Thorne CA, Hanson AJ, Schneider J, et al. Small-molecule inhibition of Wnt signaling through activation of casein kinase 1alpha. Nature chemical biology. 2011; 6(11):829–36. [PubMed: 20890287]
39. Gjorevski N, Nelson CM. Integrated morphodynamic signalling of the mammary gland. Nature reviews. 2011; 12(9):581–93.
40. Bocchinfuso WP, Hively WP, Couse JF, Varmus HE, Korach KS. A mouse mammary tumor virus-Wnt-1 transgene induces mammary gland hyperplasia and tumorigenesis in mice lacking estrogen receptor-alpha. Cancer research. 1999; 59(8):1869–76. [PubMed: 10213494]
41. Song N, Schwab KR, Patterson LT, et al. pygopus 2 has a crucial, Wnt pathway-independent function in lens induction. Development (Cambridge, England). 2007; 134(10):1873–85.
42. Schwab KR, Patterson LT, Hartman HA, et al. Pygo1 and Pygo2 roles in Wnt signaling in mammalian kidney development. BMC biology. 2007; 5:15. [PubMed: 17425782]
43. Visvader JE. Cells of origin in cancer. Nature. 2011; 469(7330):314–22. [PubMed: 21248838]
44. Herschkowitz JI, Simin K, Weigman VJ, et al. Identification of conserved gene expression features between murine mammary carcinoma models and human breast tumors. Genome biology. 2007; 8(5):R76. [PubMed: 17493263]
45. Gupta PB, Fillmore CM, Jiang G, et al. Stochastic state transitions give rise to phenotypic equilibrium in populations of cancer cells. Cell. 2011; 146(4):633–44. [PubMed: 21854987]
46. Li B, Rheaume C, Teng A, et al. Developmental phenotypes and reduced Wnt signaling in mice deficient for pygopus 2. Genesis. 2007; 45(5):318–25. [PubMed: 17458864]
47. Sun P, Yuan Y, Li A, Li B, Dai X. Cytokeratin expression during mouse embryonic and early postnatal mammary gland development. Histochemistry and cell biology. 2010; 133(2):213–21. [PubMed: 19937336]
48. Guo W, Lasky JL, Chang CJ, et al. Multi-genetic events collaboratively contribute to Pten-null leukaemia stem-cell formation. Nature. 2008; 453(7194):529–33. [PubMed: 18463637]
49. Subramanian A, Tamayo P, Mootha VK, et al. Gene set enrichment analysis: a knowledge-based approach for interpreting genome-wide expression profiles. Proceedings of the National Academy of Sciences of the United States of America. 2005; 102(43):15545–50. [PubMed: 16199517]
50. LaMarca HL, Visbal AP, Creighton CJ, et al. CCAAT/enhancer binding protein beta regulates stem cell activity and specifies luminal cell fate in the mammary gland. Stem cells (Dayton, Ohio). 2010; 28(3):535–44.
51. Hu Y, Smyth GK. ELDA: extreme limiting dilution analysis for comparing depleted and enriched populations in stem cell and other assays. Journal of immunological methods. 2009; 347(1–2):70–8. [PubMed: 19567251]
52. Cicalese A, Bonizzi G, Pasi CE, et al. The tumor suppressor p53 regulates polarity of self-renewing divisions in mammary stem cells. Cell. 2009; 138(6):1083–95. [PubMed: 19766563]
53. Karantza-Wadsworth V, White E. A mouse mammary epithelial cell model to identify molecular mechanisms regulating breast cancer progression. Methods in enzymology. 2008; 446:61–76. [PubMed: 18603116]
54. Eustice DC, Feldman PA, Colberg-Poley AM, Buckery RM, Neubauer RH. A sensitive method for the detection of beta-galactosidase in transfected mammalian cells. Biotechniques. 1991; 11(6): 739–40. 42–3. [PubMed: 1809326]

Author Manuscript
Author Manuscript
Author Manuscript
Author Manuscript

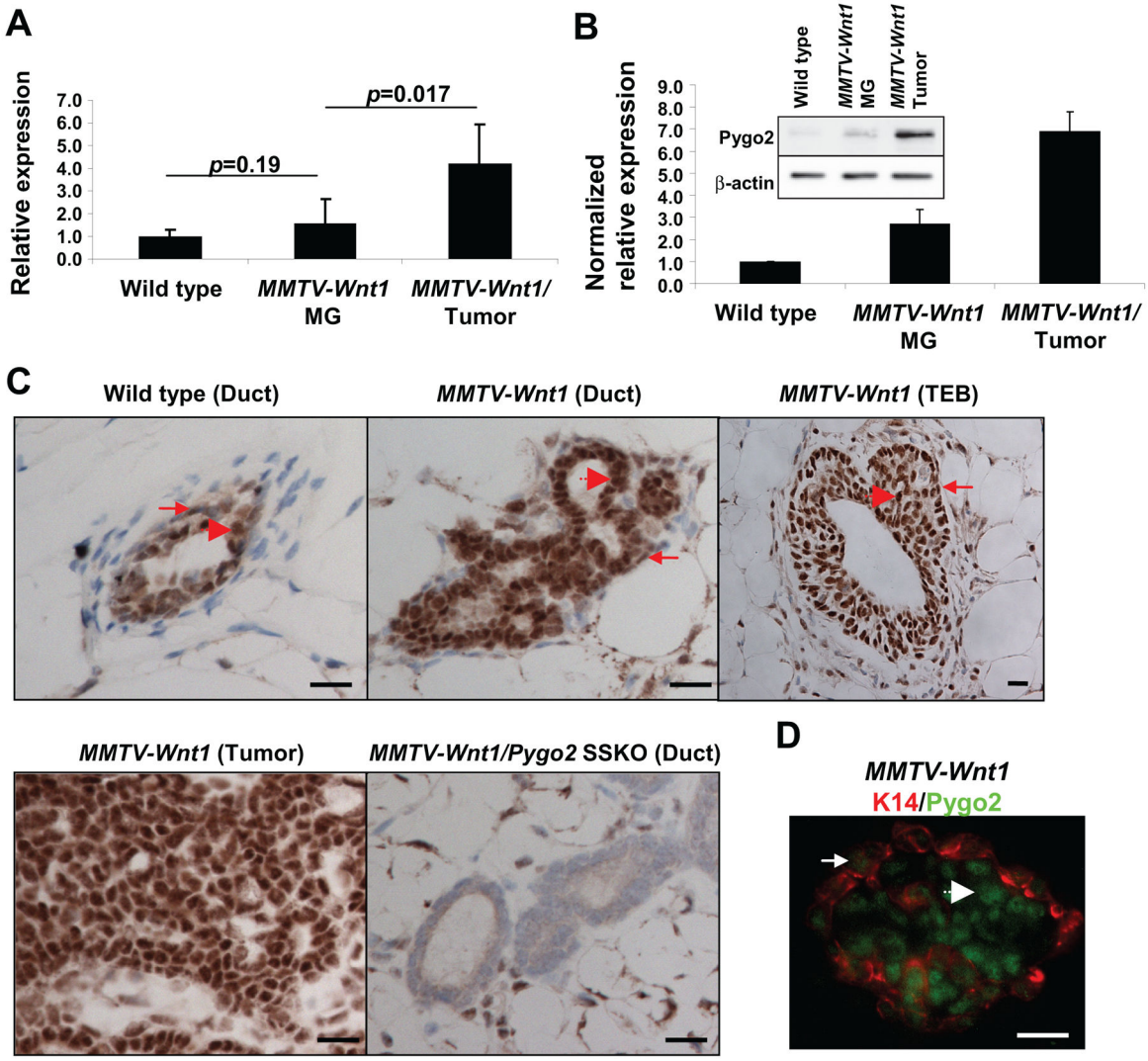

Figure 1. Elevated expression of Pygo2 in MGs and tumors of *MMTV-Wnt1* females

(A) RT-qPCR analysis showing elevated levels of *Pygo2* mRNA in *MMTV-Wnt1* MG and tumor cells (n=4). Non-tumorous MGs and tumor tissues were obtained from tumor-bearing *MMTV-Wnt1* mice (4–8 month old). Age-matched wild-type FVB/N mice were used as controls (n=4). Data were normalized against *GAPDH* mRNA level. (B) Elevated level of Pygo2 protein in mammary cells isolated from *MMTV-Wnt1* MGs or tumors. Quantification was performed by densitometric analysis of Western blots (inset shows a representative example) of lysates prepared from *MMTV-Wnt1* (n=2) and control littermates (n=2) (6–7 month old). Values were normalized against β-actin, and were corrected for differences in the epithelial content of tissues of the indicated genotypes (See Supplemental Figure 1). In both (A) and (B), means ± standard deviations are shown. (C–D) Immunohistochemical (C) and indirect immunofluorescent (D) analysis of Pygo2 protein expression in tissues of the indicated genotypes. Antibody specificity was indicated by lack of signals in MGs from skin/mammary-specific *Pygo2* knockout (SSKO) mice (see below) that carry the *MMTV-Wnt1* transgene. Section in (D) was double-stained using Pygo2 (green) and K14 (red)

antibodies. Arrows and arrowheads in (C) and (D) indicate cap/basal (K14-positive) and body/luminal cells, respectively. Scale bar = 20 μm (C), 10 μm (D).

Author Manuscript Author Manuscript Author Manuscript Author Manuscript

Author Manuscript Author Manuscript Author Manuscript Author Manuscript

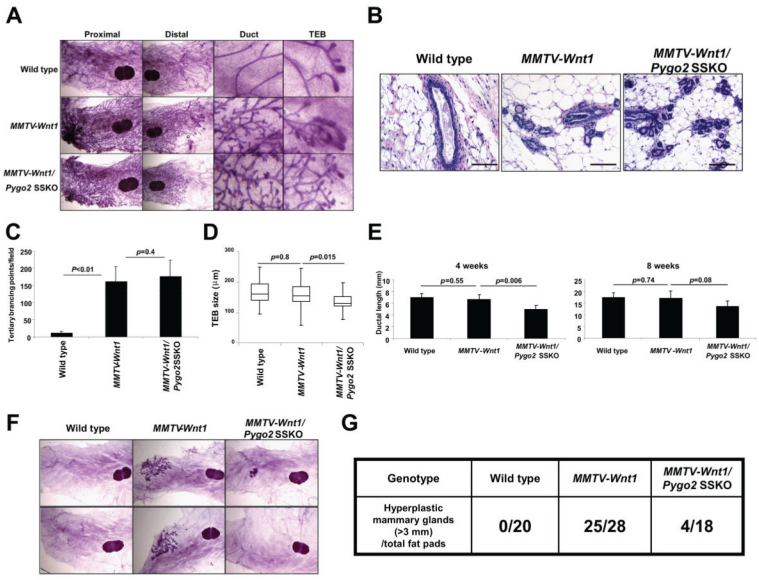

Genotype	Wild type	*MMTV-Wnt1*	*MMTV-Wnt1/ Pygo2* SSKO
Hyperplastic mammary glands (>3 mm) /total fat pads	0/20	25/28	4/18

Figure 2. Effects of *Pygo2* deletion on mammary phenotypes of the *MMTV-Wnt1* mice

(A) Representative whole-mount images of MGs from 8-week old female mice of the indicated genotypes. n=11 for *MMTV-Wnt1* and n=8 for *MMTV-Wnt1*/*Pygo2* SSKO mice. (B) H/E-stained images. Scale bar = 50 μm. (C) Quantification (means ± standard deviations) of tertiary branching. Branching points of tertiary ducts were counted for a total of 12 randomly picked fields for three mice per genotype. (D) Quantification of TEB size. Diameter of TEB was measured for a total of 24–31 TEBs from three mice per genotype. Median (middle bars), maximum-minimum value (boxes), ±1.5 interquartile range (whiskers) are shown. (E) Quantification (means ± standard deviations) of ductal length (distance between nipples and the distal tips of the growing ducts; n=5 per genotype per age). (F) Representative whole-mount images of MGs from 10-week old male mice of the indicated genotypes. (G) Incidence of hyperplastic mammary trees (larger than 3 mm in length) in #3 or #4 MGs was quantified.

Author Manuscript Author Manuscript Author Manuscript Author Manuscript

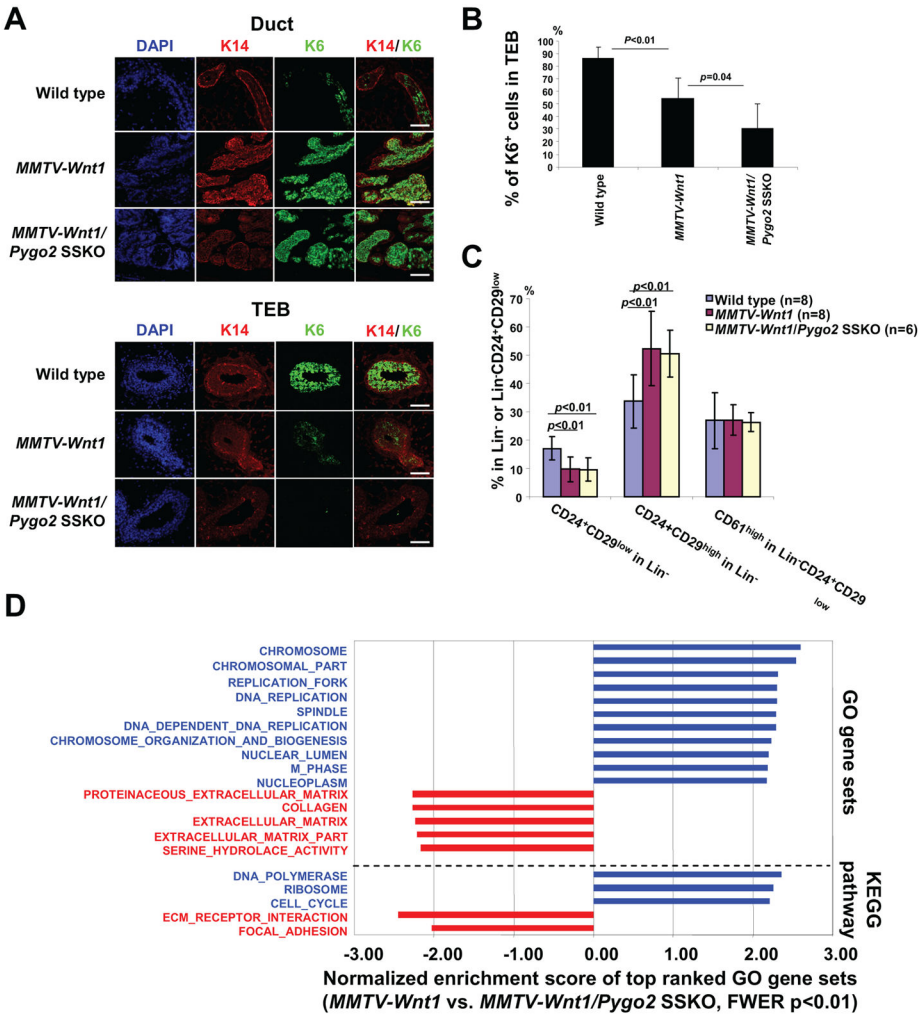

Figure 3. Effects of *Pygo2* deletion on epithelial subpopulations and gene expression in *MMTV-Wnt1* MGs

(A) Indirect immunofluorescence of K6 (green) and K14 (red) expression in MGs of 4-week old females of the indicated genotypes. DAPI (blue) stains the nuclei. Representative images of ducts (upper panels) and TEBs (lower panels) are shown. Scale bar = 20 μm. (B) Quantification (means ± standard deviations) of K6-positive mammary epithelial cells in TEB of 4-week old females. A total of six TEBs/mouse (n=2 for each genotype) were randomly picked and K6-positive/total cells counted. (C) Quantification of $Lin^{-}CD24^{+}CD29^{low}$ (luminal), $Lin^{-}CD24^{+}CD29^{high}$ (MaSC/basal), and $Lin^{-}CD24^{+}CD29^{low}CD61^{high}$ (luminal progenitor) populations in MGs of 8–10-week old female littermates of the indicated genotypes. The chart represents means ± standard deviations of the percentage of $Lin^{-}CD24^{+}CD29^{low}$ luminal population or $Lin^{-}CD24^{+}CD29^{high}$MaSC/basal population in total Lin^{-} population, and percentage of $Lin^{-}CD24^{+}CD29^{low}CD61^{high}$ luminal progenitor population in $Lin^{-}CD24^{+}CD29^{low}$total luminal population. n=8 for wild-type or *MMTV-Wnt1* mice, n= 6 for *MMTV-Wnt1*/*Pygo2* SSKO mice. (D) GSEA of Gene Ontology (GO) and KEGG pathway gene sets reveals gene expression differences in FACS-purified MaSC/basal populations from *MMTV-Wnt1* and

Author Manuscript Author Manuscript Author Manuscript Author Manuscript

MMTV-Wnt1/*Pygo2* SSKO MGs. Normalized enrichment scores for significantly enriched gene sets [family-wise error rate (FWER) $p<0.01$)] are shown. Blue and red bars indicate gene sets that are enriched in *MMTV-Wnt1* and *MMTV-Wnt1*/*Pygo2* SSKO samples, respectively.

Author Manuscript Author Manuscript Author Manuscript Author Manuscript

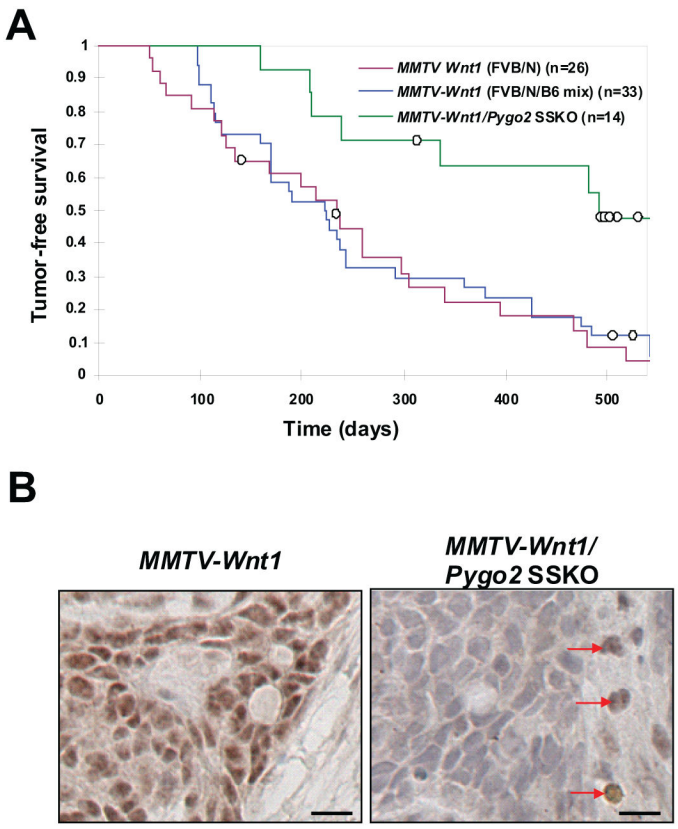

Figure 4. Effect of *Pygo2* deletion on Wnt-induced mammary tumorigenesis

(A) Kaplan-Meier analysis of tumor-free survival. *MMTV-Wnt1/Pygo2* SSKO mice were generated in a FVB/N/B6 mixed background (See Materials and Methods for details), whereas *MMTV-Wnt1* mice were analyzed in this mixed background as well as in a pure FVB/N background. $p>0.5$ for *MMTV-Wnt1* (FVB/N) vs *MMTV-Wnt1* (FVB/N/B6 mix); $p=0.007$ for *MMTV-Wnt1* (FVB/N/B6 mix) vs *MMTV-Wnt1/Pygo2* SSKO by Log-rank test. (B) Immunohistochemical analysis of Pygo2 protein in tumors from mice of the indicated genotypes. Arrows indicate Pygo2-positive stromal cells. Scale bar = 10 μm.

Author Manuscript Author Manuscript Author Manuscript Author Manuscript

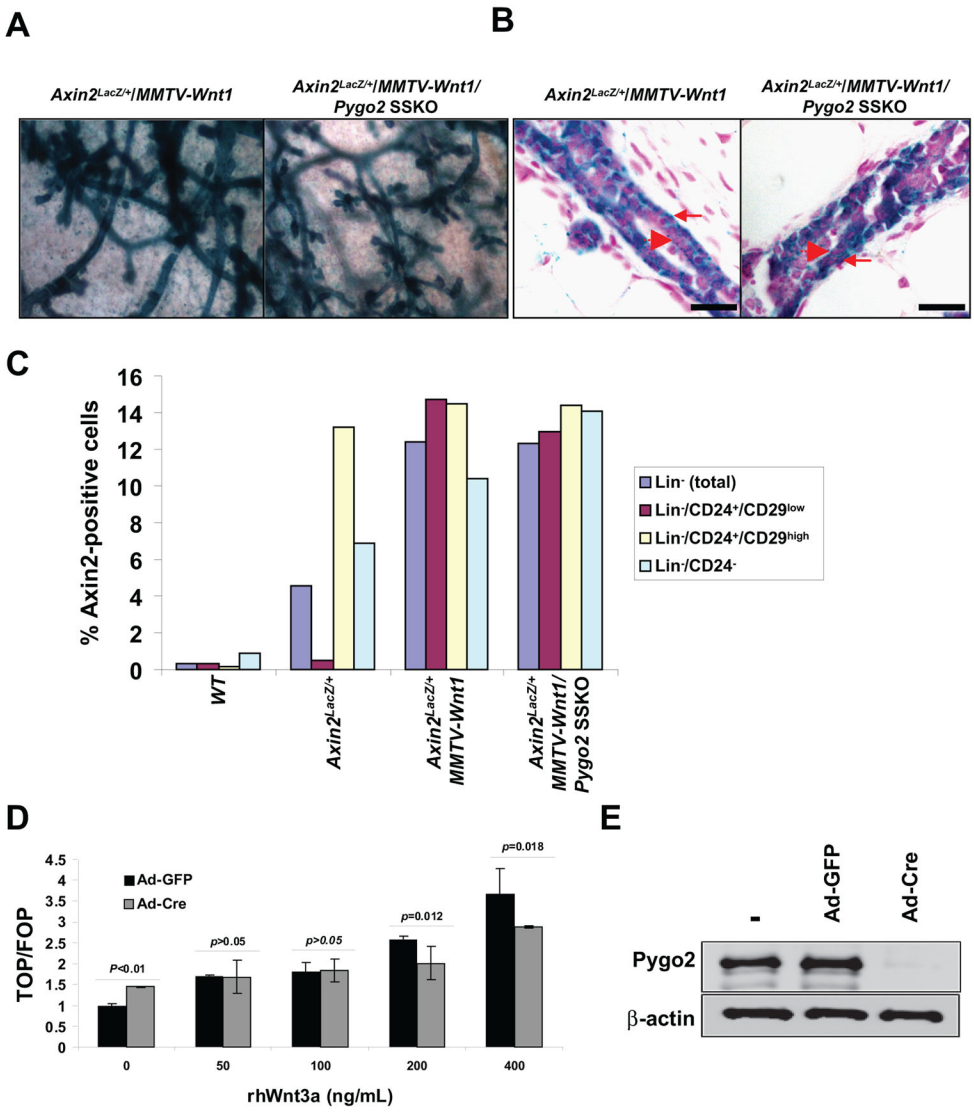

Figure 5. Effect of Pygo2 loss on canonical Wnt signaling in *MMTV-Wnt1* mammary cells

(A–B) X-gal staining of MGs from *Axin2*$^{LacZ/+}$/*MMTV-Wnt1* and *Axin2*$^{LacZ/+}$/*MMTV-Wnt1*/*Pygo2* SSKO littermates. Images of whole mount staining (A) and histological sections (B) are shown. Nuclei were counter stained with Nuclear Fast Red in (B). Arrows and arrowheads indicate LacZ-positive cells in basal and luminal layers, respectively. Scale bar = 20 μm. (C) FACS analysis of LacZ activity in epithelial subpopulations from *Axin2*$^{LacZ/+}$/*MMTV-Wnt1* and *Axin2*$^{LacZ/+}$/*MMTV-Wnt1*/*Pygo2* SSKO littermates. LacZ activity was detected using a fluorescent LacZ substrate (FDG), and the percentages of LacZ-positive cells in the indicated mammary subpopulations (visualized based on surface marker expression) are shown. (D) Pygo2 modulates TOP-Flash response of G236 cells to recombinant Wnt3a. TOP-Flash reporter activity was measured 24 hours after the addition of recombinant Wnt3a at the indicated concentrations to control (Ad-GFP) and Pygo2-deficient (Ad-Cre) G236 cells. Means ± standard deviations of a triplicate experiment are shown. Similar results were obtained from two independent experiments. (E) Pygo2 protein

Author Manuscript Author Manuscript Author Manuscript Author Manuscript

expression was analyzed by Western blotting in uninfected (−), Ad-GFP- or Ad-Cre-infected G236 cells at 30 days after infection of adenoviruses. β-actin served as a loading control.

Author Manuscript Author Manuscript Author Manuscript Author Manuscript

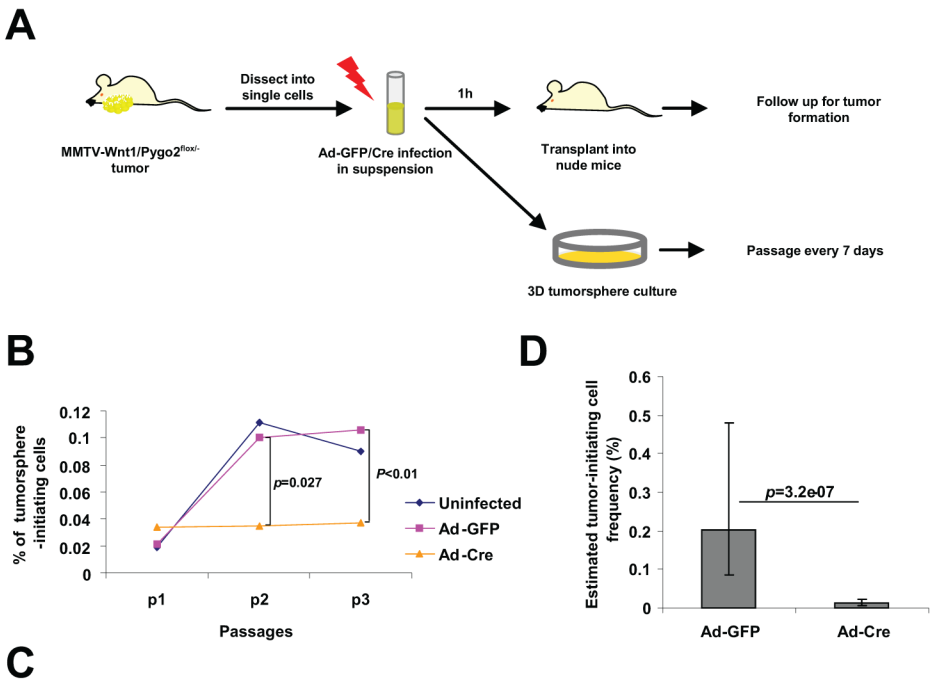

C

Cells injected	Ad-GFP	Ad-Cre
20000	N.D.	10/10
10000	6/6	4/6
2000	7/7	3/7
400	3/6	0/6
Tumor initiating cells	1/492	1/5857
95% CI	1/208-1/1164	1/3174-1/10806

Figure 6. Pygo2 regulates the tumorsphere/tumor-initiating capacity of *MMTV-Wnt1* mammary tumor cells

(A) Experimental strategy. Mammary tumor cells were freshly isolated from tumor-bearing *MMTV-Wnt1/Pygo2*$^{flox/-}$ mice and infected with the indicated adenoviruses right before tumorsphere or transplantation assays. Adenovirus infection efficiency was >80% (see text for details). (B) Reduced number of tumorsphere-initiating cells upon acute *Pygo2* deletion. Tumorspheres were passaged every 7 days. The chart represents the percentages of cells that generate tumorspheres in total cells based on the assumption that all tumorspheres generated have a clonal origin. Uninfected control was included to exclude the adverse effect of adenoviruses. *p* values were calculated from five replicates. Similar results were obtained using two independent tumors. (C–D) Estimated tumor-initiating frequency after Ad-GFP or Ad-Cre infection of *MMTV-Wnt1/Pygo2*$^{flox/-}$ primary tumor cells. Results from three independent serial dilution (ranging from 400–20,000 cells/infection) transplantation experiments using three *MMTV-Wnt1/Pygo2*$^{flox/-}$ primary tumors are summarized in (C) and a graphic representation of the estimated tumor-initiating cell frequency is shown in (D). N.D., not determined. Statistical analysis was performed as described in Materials and

Methods, with *p* value calculated as pairwise group difference (D). The error bars in (D) indicate 95% confidence intervals.

Author Manuscript Author Manuscript Author Manuscript Author Manuscript

Author Manuscript Author Manuscript Author Manuscript Author Manuscript

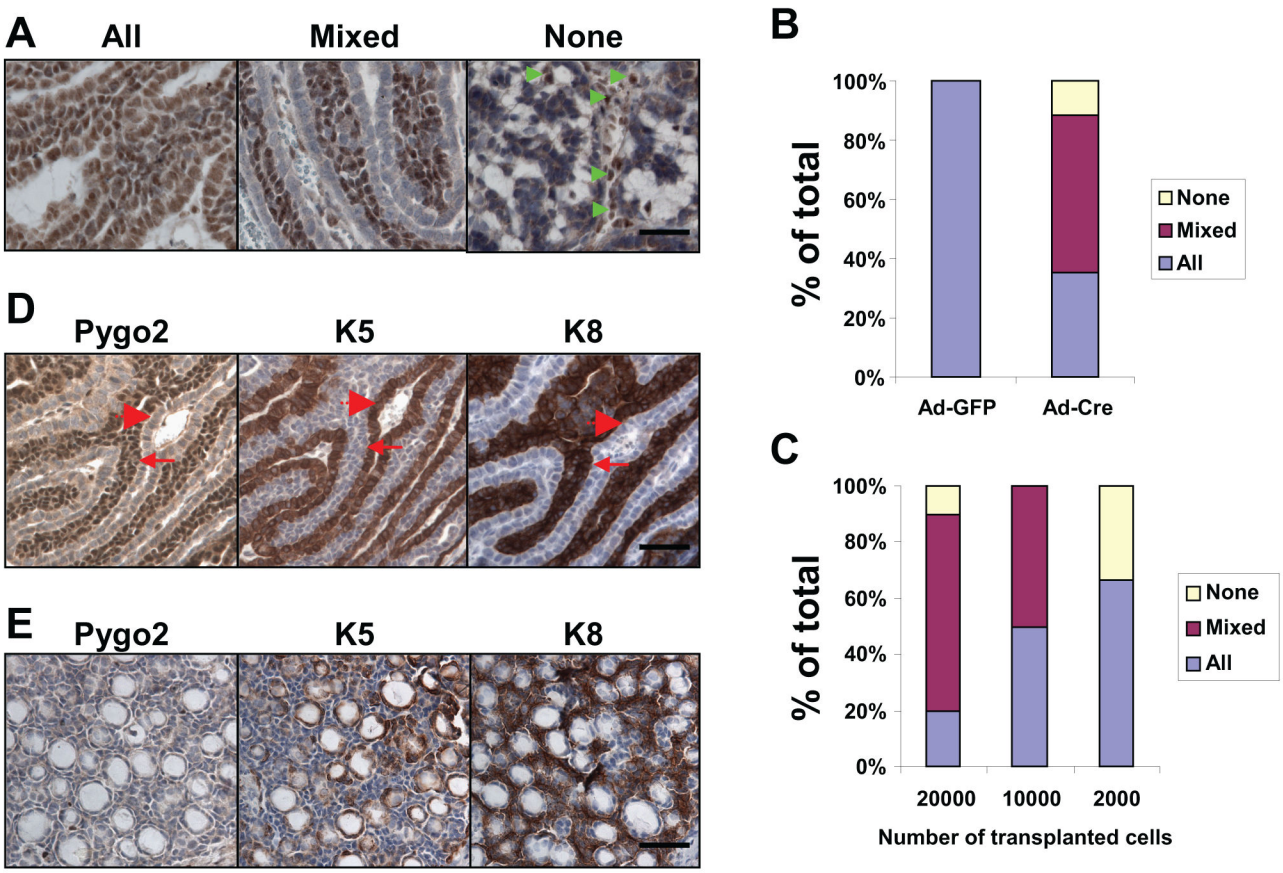

Figure 7. Competitive advantage of Pygo2-expressing cells and skewed lineage differentiation of Pygo2-deficient cells during tumor formation after transplantation

(A) Immunohistochemical analysis of Pygo2 expression in the transplanted tumors after Ade-Cre-mediated acute deletion of *Pygo2* (see Figure 6 for details). Representative images of Ad-Cre-treated tumor tissues are shown for tumors that contain only Pygo2-expressing cells ("All"), a mixture of Pygo2-expressing and Pygo2-deficient cells ("Mixed"), or no Pygo2-expressing tumor cells ("None"). Green arrowheads indicate Pygo2-positive stromal cells. (B) Quantification of the percentages of "None", "Mixed", and "All" types of tumors. Note that as a control, Ad-GFP-infected tumor cells produced only "All"-type tumors. (C) Dependence of tumor type on the number of transplanted tumor cells. Percentages of "None", "Mixed", and "All" types of tumors were quantified for the indicated numbers of Ade-Cre-treated, transplanted cells. (D) A representative "Mixed"-type tumor derived from Ad-Cre-infected tumor cells showing segregation of Pygo2-expressing and Pygo2-deficient cells in luminal and basal, respectively, compartments. Arrows and arrowheads indicate luminal ($K8^+$) and basal ($K5^+$), respectively, cells on serial sections. (E) Pygo2-deficient cells populate a microacinar section of a "Mixed"-type tumor derived from Ad-Cre-infected tumor cells. Immunohistochemistry was performed using the indicated antibodies on serial sections. Scale bars in (A), (D), (E) = 20 μm.

Author Manuscript Author Manuscript Author Manuscript Author Manuscript

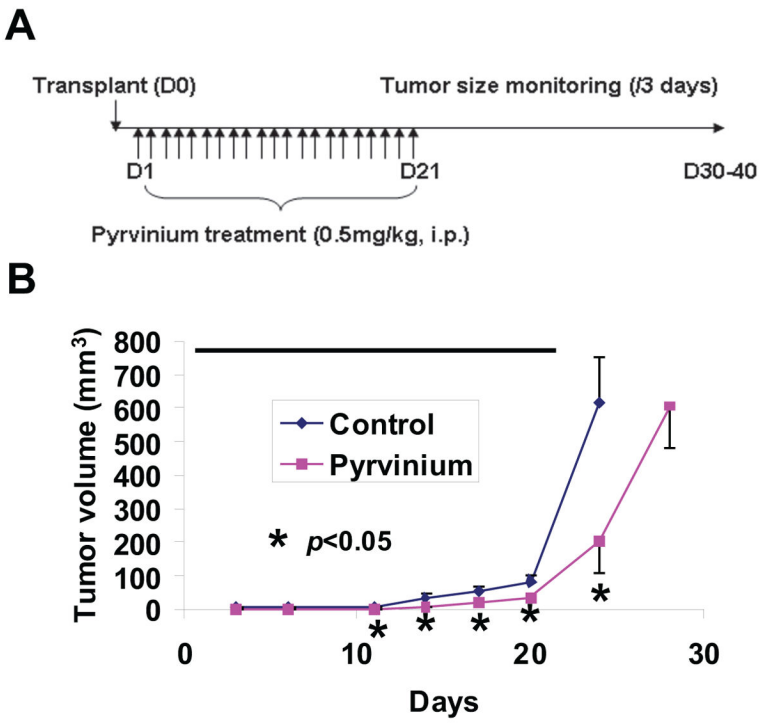

Figure 8. Effect of pyrvinium on Wnt-induced mammary tumorigenesis

(A) Experimental strategy. Single cell suspension was prepared from a primary tumor from a *MMTV-Wnt1* mouse and 1×10^5 tumor cells were bilaterally injected into #4 MGs of nude mice (D0). Mice were administered daily with pyrvinium phosphate (0.5 mg/kg) via intraperitoneal (i.p.) injection beginning at a day after transplantation (D1) and continued daily for 21 days (D1–D21) (n=10 recipient mice per condition). (B) Tumor growth curve. Tumor volume was estimated from the maximum and minimum diameters measured every 3 days by a caliper. Saline injection was performed as a control treatment.